Carbon complexes in highly C-doped GaN

John L. Lyons, Evan R. Glaser, Mary Ellen Zvanut, Subash Paudel, Malgorzata Iwinska, Tomasz Sochacki, and Michal Bockowski

Phys. Rev. B **104**, 075201 — Published 5 August 2021
DOI: 10.1103/PhysRevB.104.075201

Carbon complexes in highly C-doped GaN

John L. Lyons,[1] Evan R. Glaser,[2] Mary Ellen Zvanut,[3] Subash Paudel,[3] Malgorzata Iwinska,[4] Tomasz Sochacki,[4] and Michal Bockowski[4]
[1] *Center for Computational Materials Science, United States Naval Research Laboratory, Washington, DC 20375, USA*
[2] *Electronics Science and Technology Division, United States Naval Research Laboratory, Washington, DC 20375, USA*
[3] *Department of Physics, University of Alabama at Birmingham, Birmingham, AL 35294, USA*
[4] *Institute of High Pressure Physics Polish Academy of Sciences, Sokolowska, 29/37, 01-142 Warsaw, Poland*

(Dated: 20 July 2021)

We investigate the properties of heavily C-doped GaN grown by hydride vapor phase epitaxy (HVPE) using both optical experiments and hybrid density functional theory calculations. Previous work has established that carbon acceptors (C_N) give rise to a yellow luminescence band near 2.2 eV along with a blue luminescence band near 2.9 eV. Photoluminescence measurements show the yellow band shifting as a function of carbon concentration, suggesting a change in the behavior of carbon species as carbon content increases. With hybrid density functional theory we calculate the electrical and optical behavior of carbon centers containing multiple carbon impurities, which may arise in heavily-doped material. We compare the behavior of these complexes to the isolated centers, and find that the dicarbon donor-acceptor (C_{Ga}-C_N) complex is a candidate to explain the shift in the yellow luminescence peak. Tricarbon complexes have high formation energies and modest binding energies, and also give rise to optical transitions that are inconsistent with the observed spectra. We also identify the split dicarbon interstitial on the gallium site as a low-energy species with a large binding energy that may act to compensate carbon acceptors. Local vibrational modes are calculated for carbon impurity centers, and we compare these results to recent experiments. Dicarbon and tricarbon complexes involving C_{Ga} and C_N exhibit modes that are only slightly higher than the isolated species, while carbon interstitials and related complexes give rise to vibrational modes much higher than C_{Ga} and C_N.

I. INTRODUCTION

Carbon is among the most important contaminants and intentional dopants of GaN. Due to its presence in precursor molecules, it is often unintentionally incorporated during GaN grown with metal organic chemical vapor deposition[1] or atomic layer deposition techniques.[2] In addition to being a contaminant, C is also intentionally added to GaN to compensate donors and create semi-insulating material useful in many device designs.[3,4] Deep level transient spectroscopy (DLTS) measurements have also shown that C can act as a hole trap, compensating Mg doping in *p*-type GaN.[5] In addition to acting as a compensating center, C leads to carrier trapping that can reduce device performance, and balancing between these two behaviors will be crucial for designing future GaN-based devices.[6,7]

The electrical behavior of moderately C-doped GaN seems to be driven by the deep acceptor incorporating on the nitrogen site (C_N).[8] Because it exhibits a $(0/-)$ acceptor level $\sim$1 eV above the valence-band maximum (VBM) of GaN, C_N can lead to semi-insulating material, as indicated by recent temperature-dependent Hall measurements on C-doped GaN.[9] Vibrational spectroscopy experiments have also confirmed that C incorporates as C_N in C-doped GaN, giving rise to distinct local vibrational modes (LVMs) between 750-780 cm^{-1}.[10] Optical experiments also support the deep acceptor behavior of C_N, which was predicted[8] to give rise to the long-observed 2.2 eV yellow luminescence (YL) peak in GaN.[11]

In addition, due to a deep $(+/0)$ donor transition level, C_N was also predicted[12] to give rise to a blue luminescence (BL) peak at 2.7 eV. A combined experimental and theoretical investigation also attributed 2.2 eV YL and 2.9 eV BL signals to the two charge-transition levels of C_N, and also found that the BL band appeared mostly in heavily C-doped GaN and at high excitation intensities.[13] DLTS studies have also associated a trap 0.29 eV from the VBM with C_N,[14] indicating that C_N might be an important source of carrier compensation in *p*-type GaN, due to the presence of the $(+/0)$ donor level in the vicinity of the VBM.

More recently, questions have emerged about the behavior of carbon in heavily-doped GaN. Using hybrid functional calculations, Matsubara and Bellotti investigated the properties of C-containing complexes in GaN,[15,16] including complexes containing two C centers. In particular, they found that C_{Ga}-C_N [i.e., a complex between the carbon acceptor and a carbon donor on the gallium site (C_{Ga}), as shown in Fig. 1] had a moderate formation energy and binding energy (relative to isolated C_{Ga} and C_N) in *n*-type GaN, and exhibited donor transition levels near the GaN VBM. Deák et al. also investigated the properties of multi-carbon complexes, and found similar behavior[17].

With photoluminescence (PL), temperature-dependent Hall effect measurements, and magnetic

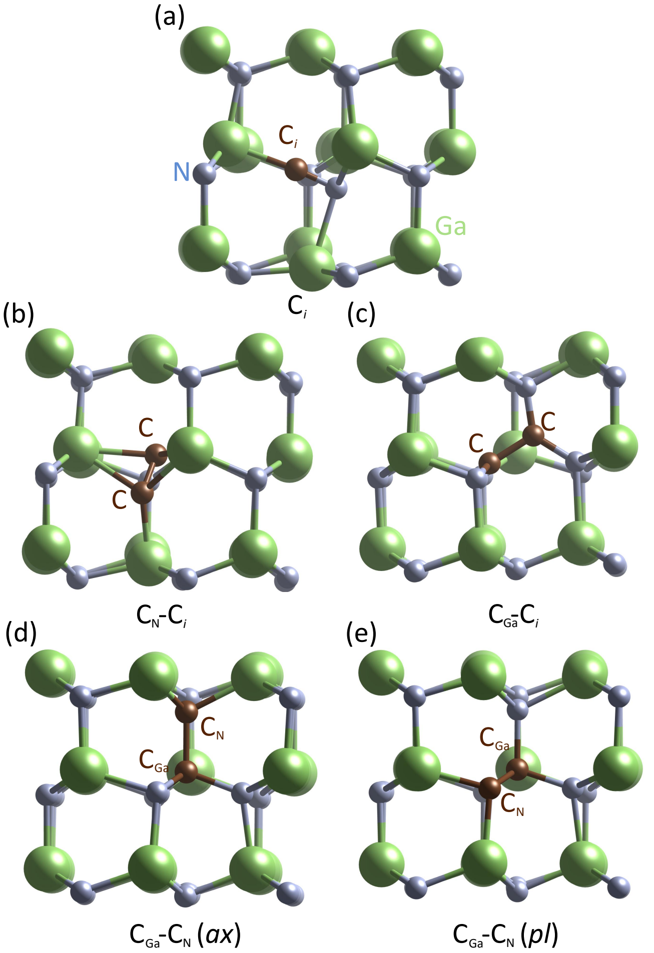

FIG. 1. Configurations of C-containing defects and complexes in GaN. In (a), the split-interstitial configuration of C_i^{2+} is shown, in (b) the $(C_N\text{-}C_i)^+$ complex, and in (c) the $(C_{Ga}\text{-}C_i)^{2+}$ complex. The C_{Ga}-C_N dicarbon complexes are shown in the (d) *ax* and (e) *pl* configurations, both in the neutral charge state.

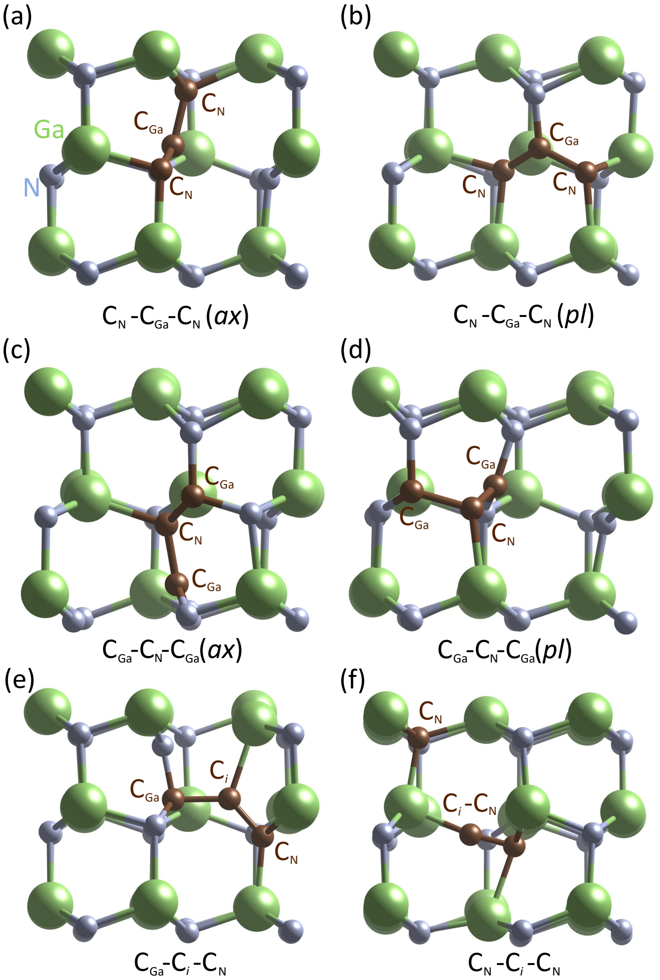

FIG. 2. Configurations of tricarbon complexes in GaN. The tricarbon C_N-C_{Ga}-C_N complexes are shown in (a) *pl* and (b) *ax* orientations, both in the negative charge state. In (c) the *pl* and (d) the *ax* orientations of the C_{Ga}-C_N-C_{Ga} complexes are shown, both in the + charge state. Also shown are two other tricarbon complexes: in (g) $(C_{Ga}\text{-}C_i\text{-}C_N)^{2+}$ and (h) $(C_N\text{-}C_i\text{-}C_N)^{2+}$.

resonance experiments, Zvanut et al. examined[18] the electronic, optical, and defect properties of HVPE-grown GaN doped with a range of C concentrations. They found that the resistivity of these samples saturated at concentrations above 2×10^{17} cm^{-3}, as did the electron paramagnetic resonance (EPR) signal of the C_N acceptor, suggesting that C_N was compensated by newly-formed defects at high levels of C doping. Furthermore, Piotrzkowski et al.[19] reported an increase in carbon compensation as its concentration was increased in GaN, and suggested that significant incorporation of C-related donors [such as C_{Ga} and carbon interstitials (C_i)] were the origin of this behavior.

Other researchers have claimed that tricarbon complexes form in both AlN and GaN heavily doped with C.[20–24] Based on vibrational spectroscopy measurements that identified a distinct LVM at 1769 cm^{-1} in C-doped AlN, Irmscher et al. proposed[20] that a tricarbon C_N-C_{Al}-C_N complex was forming in this material. Later studies found similar high-wavenumber LVMs in C-doped GaN, which was attributed to the presence of analogous C_N-C_{Ga}-C_N tricarbon centers (with the counterpart C_{Ga}-C_N-C_{Ga} complexes suggested to occur in less significant concentrations).[21,22,25] Examples of such complexes are shown in Figs. 2a-d. To our knowledge, the stability and electronic properties of this type of tricarbon complex has not been evaluated by first-principles calculations.

Here we investigate heavily C-doped GaN using a combination of experiments and density functional theory (DFT) calculations. PL measurements indicate that the YL peak blueshifts as C concentration increases, while the BL peak decreases in intensity. Optically-detected magnetic resonance (ODMR) experiments confirm that the C_N acceptor is participating in the YL process, and suggest that a similar center (likely C_N^+) is participating in the BL. DFT calculations on a set of C-containing species indicate that C_{Ga}-C_N are a likely candidate for causing the shift in the YL band as C content increases. Complexes containing three C atoms (which have been proposed previously) do have modest binding energies (but high formation energies), and their optical properties are not consistent with experiment. We also calculate LVMs of C-containing centers, and find that the dicarbon and tricarbon complexes give rise to C-related LVMs only slightly higher than isolated C_N or C_{Ga}. LVMs exceeding 1700 cm^{-1} are only predicted for species involving C_i, but not for the tricarbon complexes as had been proposed previously.[21,22]

II. EXPERIMENTAL AND THEORETICAL METHODS

The PL and ODMR experiments were performed on C-doped GaN grown by HVPE on high-quality ammonothermal GaN seeds and subsequently removed from those seeds via mechanical polishing to form free-standing 250-500 micron-thick substrates. The substrates were intentionally doped with carbon impurities by adjusting the CH_4 flow rate in the growth reactor zone. Additional growth details are given elsewhere.[9] We note that these PL and ODMR defect characterization studies were all done on the same 2 mm x 6 mm size samples diced from their parent carbon-doped GaN substrates. Secondary ion mass spectroscopy (SIMS) of these GaN substrates revealed C doping levels from 2 x 10^{17} – 1 x 10^{19} cm^{-3} and a uniform depth profile over the top 6 microns. Also, SIMS showed evidence for two common residual shallow donor (SD) impurities, with Si in the range of 2-6 x 10^{17} cm^{-3} and oxygen between 1 and 3 x 10^{17} cm^{-3}, as well as residual Mg (acceptor) impurities with concentrations of 3-7 x 10^{15} cm^{-3}. In addition, EPR[18] of these same samples and detailed variable temperature (455-1000 K) Hall effect transport measurements[19] on sister substrate samples were also recently published. Most notably, both the EPR and transport studies revealed evidence for increasing concentrations of compensating donor species with increasing C doping levels.

The optical recombination processes in the GaN:C samples were investigated by PL spectroscopy at 2 K. The PL was excited with the 351 nm line from an Ar ion laser. The emission was analyzed by a 0.25 m double-grating spectrometer and detected by a UV-enhanced GaAs photomultiplier tube. In addition, the nature and possible origin(s) of the radiative recombination observed from these samples were further probed using ODMR spectroscopy. The ODMR experiments at 1.6 K were performed in a 24 GHz spectrometer with the samples placed in the tail section of the same optical cryostat employed for the PL studies. The ODMR signal corresponds to the change in the PL intensity detected by a Si photodiode that was coherent with the on-off amplitude modulation (∼700 Hz) of 50 mW of microwave power while sweeping a dc magnetic field up to 1.1 T. Finally, the emission bands discussed below were separately analyzed via the ODMR technique by placing a combination of visible long-wavelength cutoff and/or bandpass filters in front of the Si photodiode.

Our calculations are based on DFT[26] using the hybrid functional of Heyd, Scuseria, and Ernzerhof (HSE)[27,28] as implemented in the VASP code[29] and projector-augmented waves.[30] Semicore Ga 3d electrons are treated as valence states, which has been reported to be necessary for the accurate description of carbon complexes.[15] We perform defect calculations using a 96-atom supercell, a plane-wave basis set with a cutoff of 400 eV, and a 2×2×2 Monkhorst-Pack k-point set.[31] The mixing parameter for the Hartree-Fock potential is set to 0.28 for GaN, resulting in a band gap that is in close agreement with the experimental values[15] for this computational methodology.

The stability of an impurity species in a crystal is determined by the formation energy. For example, with C on the N site in GaN in charge state q (C_N^q), the formation energy can be written as:[32]

$$\begin{aligned} E^f(C_N^q) = E_{tot}(C_N^q) - E_{tot}(\mathrm{GaN}) + \mu_N - \mu_C \\ +q(E_F + \varepsilon_v) + \Delta^q, \end{aligned} \tag{1}$$

where $E_{tot}(C_N^q)$ is the total energy of a supercell with C_N^q in charge state q, and $E_{tot}(\mathrm{GaN})$ is the total energy of the pristine supercell without a defect. Electrons added or removed from the supercell are exchanged with the Fermi level (E_F) that is referenced to the valence-band maximum (VBM; ε_v). Δ^q corresponds to a correction for the finite size of charged supercells, and is obtained using the procedure outlined in Refs. 33 and 34. More details on defect calculations for gallium nitride are discussed in Ref. 35.

Atoms added or removed from the supercell are exchanged with a reservoir whose energy is given by the chemical potential of that species. In Eq. 1, μ_N is referenced to half the energy of the N_2 molecule at $T = 0$ K, while μ_C is referenced to the energy of one C atom in the diamond phase. For defects involving Ga, μ_{Ga} is given by the energy of an atom in bulk Ga metal. μ_N and μ_{Ga} are limited in range by the enthalpy of formation of bulk GaN; i.e., they obey the relation $\mu_N + \mu_{Ga} = \Delta H_f(\mathrm{GaN})$ (which is calculated to be −1.34 eV). For instance, μ_N can vary from 0 eV (N-rich conditions) to −1.34 eV (Ga-rich conditions).

Defect LVMs are calculated using the finite difference method as implemented in VASP, using a displacement of 0.015 Å and two displacements in each direction for each ion. In all cases, only the atoms involved in the defect or defect complex and their nearest neighbors are displaced in the calculation of the Hessian matrix.

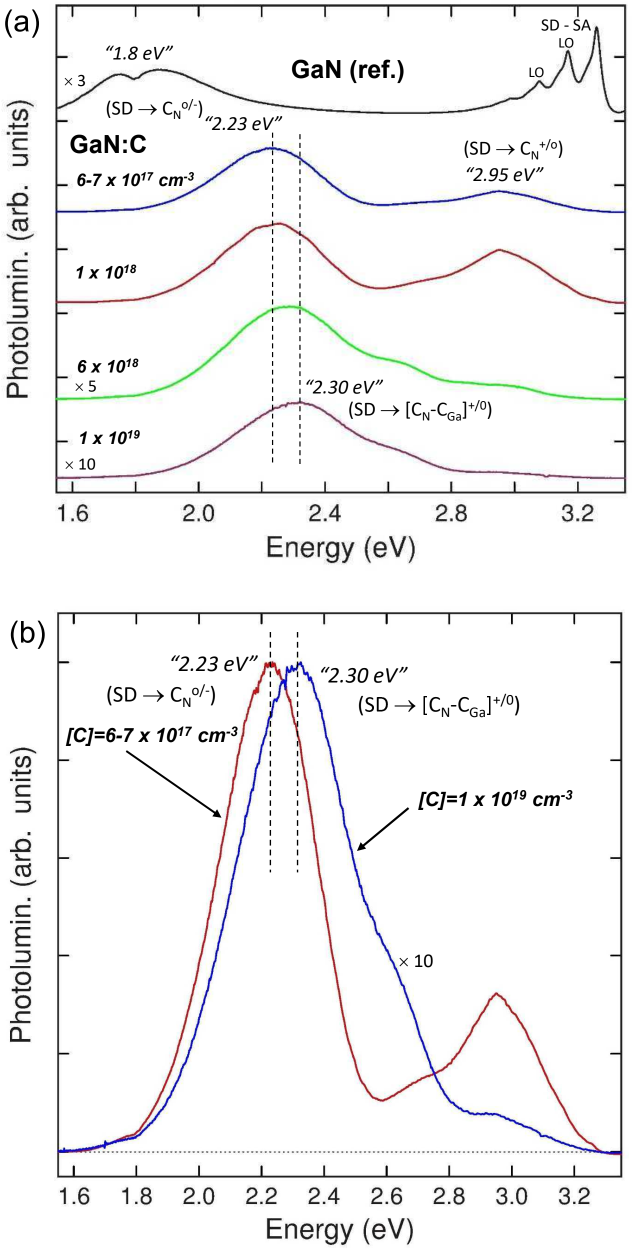

FIG. 3. (a) PL spectra of GaN samples with varying concentrations of C impurities, along with a reference sample (in black, at top). The YL near 2.2-2.3 eV is attributed to recombination into the (0/−) level of $\mathrm{C_N}$, while the BL near 2.9 eV is attributed to recombination involving the (+/0) level of $\mathrm{C_N}$. (b) Comparison between the YL peaks in lightly C-doped (6×10^{17} cm^{-3}) and highly C-doped (1×10^{19} cm^{-3}) GaN samples. The vertical dashed lines indicate the change in the peak energy of the "yellow" PL band with increasing carbon doping level.

III. RESULTS AND DISCUSSION

A. Experiments

The PL spectra observed at 2 K from 1.55 to 3.35 eV for several GaN bulk samples doped intentionally with carbon at concentrations from 6-7 x 10^{17} – 1 x 10^{19} cm^{-3} and for an (undoped) n-type GaN reference sample are shown in Fig. 3. The evolution of the PL spectra with increasing carbon doping level displayed in Fig. 3a were discussed in detail in a recent paper by M. E. Zvanut et al.[18] We highlight here some notable characteristics.

First, the main emission bands are a strong broad "yellow" PL band with peak energy at 2.23 eV that first appeared from the GaN substrate with C doping level of 2 x 10^{17} cm^{-3} (as shown in Fig. 4 from Ref. 18) and a less intense (but similarly broad) "blue" emission band with peak energy at 2.95 as shown in Fig. 3a for two intermediate C-doped GaN samples. These PL bands are ascribed[12,13] to optical processes involving shallow donors and different charge states of $\mathrm{C_N}$ deep acceptors. In particular, in the dark and with [C] ≤ [SD], as for the GaN sample with carbon doping level of 2 x 10^{17} cm^{-3} whose PL is shown in Fig. 4 of Ref. 18, some fraction of the (neutral) shallow donors are ionized while all of the (neutral) deep $\mathrm{C_N}$ centers are compensated (i.e., $\mathrm{C_N^0} \rightarrow \mathrm{C_N^-}$). In the presence of electrons (e) and holes (h) created by the above bandgap photo-excitation, the 2.23 eV "yellow" PL band arises from the following radiative recombination process:

$$(\mathrm{SD})^+ + \mathrm{C_N}^- + h\nu_{\mathrm{exc.}} \xrightarrow{(e,h)} (\mathrm{SD})^0 + \mathrm{C_N}^0 \rightarrow (\mathrm{SD})^+ + \mathrm{C_N}^- + h\nu_{\mathrm{PL}}\ (2.23\ \mathrm{eV}). \qquad (2)$$

In the dark and with $[\mathrm{C_N}] \geq$ [SD], some fraction of the neutral $\mathrm{C_N}$ deep acceptors will be compensated and some of the $\mathrm{C_N}$ centers will remain in their neutral charge state. It is those neutral $\mathrm{C_N}$ acceptors that are involved in the 2.95 eV "blue" emission band via the following optical process:

$$(\mathrm{SD})^+ + \mathrm{C_N}^0 + h\nu_{\mathrm{exc.}} \xrightarrow{(e,h)} (\mathrm{SD})^0 + \mathrm{C_N}^+ \rightarrow (\mathrm{SD})^+ + \mathrm{C_N}^0 + h\nu_{\mathrm{PL}}\ (2.95\ \mathrm{eV}). \qquad (3)$$

Thus, the simultaneous observation of the 2.23 eV "yellow" and 2.95 eV "blue" PL bands from the two GaN samples with intermediate carbon doping levels of 6-7 x 10^{17} and 1 x 10^{17} cm^{-3} (as shown in Fig. 3a) is well-described by Eqs. 2 and 3, where [C] ≥ [SD] in both samples. However, for higher doping levels of carbon, the energy of the peak in the "yellow" spectral region shifts to 2.30 eV (denoted by the vertical dotted lines), while the intensity of the 2.95 eV "blue" emission band significantly decreases relative to that of this "yellow" emission. These two attributes are highlighted in Fig. 3b, where the PL observed from intermediate and highly C-doped

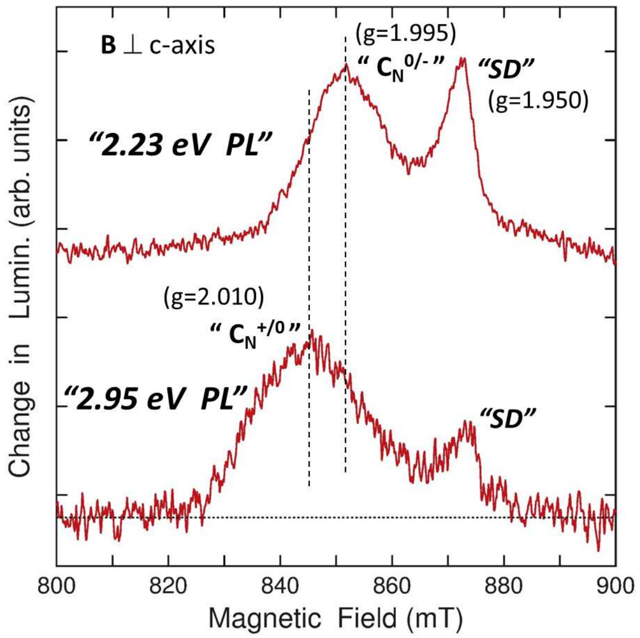

FIG. 4. ODMR on a moderately C-doped (1×10^{18} cm^{-3}) GaN sample. In the upper spectrum, ODMR indicates that the C_N (0/−) transition level is participating in the YL emission, along with a shallow donor (SD). The lower spectrum indicates that a different transition level [which we assign to C_N (+/0)] is participating in the BL emission, and that the SD is also involved.

GaN samples are normalized to the peak amplitude of the "yellow" emission. Very similar PL spectra were recently reported[9,36] for these same highly C-doped (i.e., $\geq$ 6 x 10^{18} cm^{-3}) GaN samples, and by another group for similar HVPE-grown, highly C-doped GaN substrates.[22] However, we note that the peak emission energy of the 2.2 eV "yellow" PL band did not change in MBE- and MOVPE-grown samples[37–40] with high C-doping levels (1-4 x 10^{19} cm^{-3}), as was observed in the HVPE-grown C-doped GaN samples.

We will propose below that another carbon-containing defect species (a C_{Ga}-C_N dicarbon complex) emerges with increasing carbon doping levels that can account for this "new" 2.3 eV yellow emission band. This deep donor defect can also at least partially account for the saturation at these high carbon doping levels of the EPR signal associated with paramagnetic C_N acceptor centers and for the systematic decrease of free holes for GaN samples with increasing carbon concentration revealed from temperature-dependent Hall effect measurements.[19]

ODMR spectra obtained at 24 GHz on the 2.23 eV "yellow" and 2.95 eV "blue" emission bands from the GaN bulk sample doped with a carbon impurity concentration of 10^{18} cm^{-3} are shown in Fig. 4. Two luminescence-increasing signals are observed on each PL band with the magnetic field perpendicular to the c-axis. The first (labeled SD) is common to each spectrum, and is characterized by a Zeeman splitting g-value of 1.950 and a full-width at half-maximum (FWHM) linewidth of 6-7 mT. This resonance is a well-known "fingerprint" of shallow donors, based on earlier EPR studies of n-type GaN.[41] As revealed by SIMS measurements, both the Si and O residual impurities are likely responsible for this signal, and it has not been possible to distinguish them based on magnetic resonance parameters alone.

The second ODMR feature found on the 2.23 eV emission band has a g-value of 1.995 ± 0.002 and a FWHM linewidth of $\sim$16 mT, as determined from a fit of the spectrum using Gaussian lineshapes. These parameters are identical, within error, to those found by several groups[42–46] for the deep acceptor center involved in the 2.2 eV "yellow" PL band frequently observed from unintentionally doped (n-type) GaN. We assign this resonance to the (0/−) deep acceptor transition level of the C_N defect based on the strong correlation of the 2.2 eV emission with C doping and the theoretical modeling[8] described above for this radiative recombination process.

The second ODMR signal observed on the 2.95 eV "blue" emission band is characterized by slightly different resonance parameters with a g-value of 2.010 ± 0.002 and a FWHM linewidth of $\sim$20 mT as determined again from a fit of the spectrum. We tentatively assign this resonance to the (+/0) deep donor transition level of C_N based on the modeling described above (see Eq. 3) for the broad 2.95 eV 'blue" PL band. We note that this charge state of the C_N defect is predicted[12] to have spin S=1, but only a single resonance was observed without evidence of a so-called zero field splitting behavior. One possible interpretation is that the zero-field splitting value (D) is so small that two lines could not be resolved, given the overall broad linewidth of the resonance.

Finally, ODMR has not been found to date on the broad 2.30 eV "yellow" PL band observed from the GaN sample with a C-doping level of 10^{19} cm^{-3}. More work is needed, but this may reflect a radiative lifetime of less than 100 ns associated with this emission at these high-C doping levels, given that only processes with longer lifetimes typically yield ODMR signals for the maximum microwave powers employed in these experiments.

B. Calculations

1. Electronic properties and configurations of carbon-containing species

The HSE-calculated formation energies for C-related defects are shown in Fig. 5 in N-rich conditions. Results similar to those shown in Fig. 5a (for species containing one C) have been reported previously,[8,12] for C_N, C_{Ga}, and C_i. C_N acts as a deep acceptor, giving rise to a (0/−) transition level at 0.9 eV in addition to a deep (+/0) donor level at 0.3 eV above the VBM. C_N exhibits C−Ga bonds, slightly shorter than 2 Å, that are similar to the bulk GaN length. C_{Ga} is a shallow donor, stable

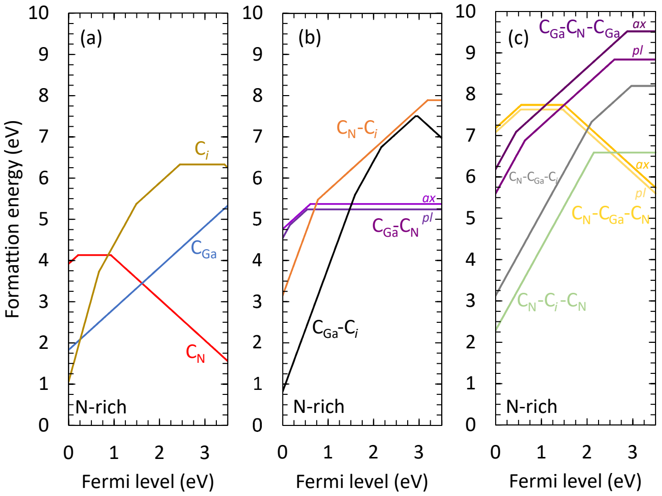

FIG. 5. Formation energy versus Fermi level for C-related defects and complexes in GaN, under N-rich conditions and calculated with HSE. In (a), species containing one carbon are shown: C_{Ga}, C_N, and C_i. In (b), complexes with two carbon are shown: C_{Ga}-C_N (in *pl* and *ax* configurations), C_N-C_i, and C_{Ga}-C_i. In (c), complexes with three carbons are shown: C_N-C_{Ga}-C_N (in *pl* and *ax* configurations), C_{Ga}-C_N-C_{Ga} (in *pl* and *ax* configurations), C_N-C_i-C_N and C_N-C_{Ga}-C_i.

only in the + charge state across the band gap of GaN, which exhibits ∼1.5 Å C−N bonds much shorter than the bulk bond lengths of GaN. Differences with previous calculations[17,47] of C_N are likely due to the choice of pseudopotential, functional, and charge-state correction scheme.

C_i acts as a deep donor stable in a number of charge states and configurations. In agreement with Ref. 15, we find that C_i can be stable in the 4+ charge state, in which it is most stable at the octahedral interstitial site (this configuration was not explored in Ref. 12). We calculate transition levels of 0.67 eV above the VBM for the (4+/2+) level of C_i, 1.49 eV for the (2+/+) level, 2.45 eV for the (+/0) level, and 3.43 eV for the (0/−) level that are in close agreement with Ref. 15. In the 2+, +, 0, and − charge states, C_i incorporates as a split interstitial, a configuration that involves a short C−N bond, as shown in Fig. 1a. The length of this bond is charge-state dependent, increasing from 1.17 Å for 2+ to 1.37 Å for the − charge state. In other words, as more electrons are added to the defect states of C_i, the C−N bond length of the split interstitial increases. Similar behavior was reported for analogous C_i split interstitials in ZnO.[48] As in Ref. 48, we here link the increase in C−N bond length to the occupation of the C_i-related antibonding orbitals.

The formation energies of the complexes containing two C atoms are shown in Fig. 5b. In agreement with Ref. 15, we find that the C_N-C_i complex can be stable in the 3+, 1+, and 0 charge states, depending on the position of the Fermi level. We find a (3+/+) transition level at 0.78 eV and a (+/0) level 3.19 eV above the VBM, which are also similar to the levels reported in Refs. 15 and 17 (the quantitative differences with Ref. 17 can be explained by the different choice of HSE parameters). For the 3+ charge state, one C atom occupies the N site, while the other acts as an interstitial, binding to C_N and to two nearby N neighbors. For $(C_N\text{-}C_i)^{3+}$, the C−C distance is 1.43 Å. As shown in Fig. 1b, we find for the + and 0 charge states that the lowest-energy configuration is a split interstitial, with the two C atoms closely bound and occupying an N site. As was the case for C_i, the C−C bond length of the C_N-C_i split interstitial increases as electrons are added to the system, going from 1.23 Å in the + charge state to 1.29 Å for the 0 charge state.

Formation energies of the C_{Ga}-C_i complex are also shown in Fig. 5b. Such a complex was also explored by Matsubara and Bellotti[15], and a similar complex has also been reported in alkaline-earth zirconates.[49] In agreement with Ref. 15, we find that this complex can be stable in the charge states from 3+ to −1. It gives rise to four charge state transition levels in the gap: a (3+/2+) level at 1.59 eV, a (2+/+) level at 2.17 eV, a (+/0) level at 2.92 eV, and a (0/−) level at 2.97 eV. The structure of this complex is split interstitial (as shown in Fig. 1c, with the two C atoms forming a close bond (its variation with charge state is shown in Table I), and each forming bonds with two neighboring N atoms. (In Ref. 15 the same configuration was found, and was referred to as *“Type 3 Split C−C”*.) While all dicarbon complexes have relatively high formation energies under *n*-type conditions, the C_{Ga}-C_i complex has the lowest formation energy (0.82 eV) among all defects considered here when the Fermi level is near the VBM.

Results for the C_{Ga}-C_N dicarbon complexes are also shown in Fig. 5b. We consider two configurations, one with both C atoms sitting in the plane perpendicular to the *c* direction [which we refer to as planar (*pl*)] and another with the C-C bond oriented along *c* [which we refer to as axial (*ax*)]. These complexes are shown in Figs. 1d and e, respectively. Despite the different orientations of these complexes, they share similar electronic properties and overall formation energies [the E^f of axial and planar $(C_{Ga}\text{-}C_N)^0$ differ by only 0.12 eV]. These complexes are neutral over most of the GaN band gap, as would be expected from the combination of C_N^- and C_{Ga}^+, and give rise to two defect levels: a (2+/+) level and a (+/0) level. For the axial complex, the (2+/+) level is coincident with the VBM, and the (+/0) level is 0.70 eV above the VBM. For the planar configuration, the (2+/+) level is 0.11 eV above the VBM while the (+/0) level is at 0.53 eV. As with isolated C_N, these levels are composed of C 2*p* orbitals stemming from the C_N member of the complex. These results are in close agreement with Ref. 15. While the thermodynamic transition levels are similar to those reported in Ref. 17, the absolute formation energies reported here are larger. This may be due to the choice in chemical potential reference for C, which was not discussed in Ref. 17. We also note that the formation energies of the dicarbon complexes are significantly higher than those containing a single carbon (e.g., C_N, C_{Ga}, and C_i). However, as noted in Ref. 25, it is possible that multi-carbon complexes are incorporated at the growth surface, and are frozen in during growth.

For C_{Ga}-C_N, both C atoms of the dicarbon complexes remain in the vicinity of their substitutional lattice sites. They feature a short C−C bond that varies with charge state, from 1.58 Å for $(C_{Ga}\text{-}C_N)^0$ to 1.54 Å for the 2+ charge state (as shown in Table I). The C−N bonds associated with the C_{Ga} member of the complex remain near 1.5 Å, while the C−Ga bonds associated with the C_N member remain near 2 Å.

Formation energies of the tricarbon complexes (C_N-C_{Ga}-C_N, C_{Ga}-C_N-C_{Ga}, C_N-C_i-C_N and C_{Ga}-C_i-C_N) are shown in Fig. 5c. As can be seen in comparison with Fig. 5b, these tricarbon complexes have generally higher formation energies than both the isolated single carbon centers (C_{Ga}, C_N, and C_i) and the dicarbon complexes (C_N-C_{Ga} and C_N-C_i). These higher formation energies indicate that the tricarbon complexes would not be expected to form as easily as the impurity centers with fewer C atoms.

C_N-C_{Ga}-C_N complexes exhibit behavior similar to the isolated C_N acceptor: they feature three charge states (+, 0, and −) and two transition levels [((+/0) and (0/−)]. Again we find that the *ax* and *pl* configurations have very similar properties, as their formation energies vary by less than 0.15 eV for any particular charge state. Their thermodynamic transition levels are also quite similar: for *ax* we find a (+/0) level at 0.56 eV and a (0/−) level at 1.50 eV, while for *pl* these levels are at 0.55 eV and 1.47 eV, respectively.

Unlike for the dicarbon complexes, we find significant off-site relaxations for the C_N-C_{Ga}-C_N complexes. As shown in Figs. 2a and b, for both *ax* and *pl* C_N-C_{Ga}-C_N complexes the C_{Ga} moves off the Ga site to become three-fold coordinated. This C atom forms two C−C ∼1.5 Å bonds with the two other C atoms of the complex, along with a similar bond with a neighboring N atom. The distance from the displaced C_{Ga} to the fourth neighboring N (a nearest neighbor before the displacement) increases to ∼2.6 Å, roughly a 33% increase over the GaN bulk bond length. This configuration resembles the one reported in Ref. 25.

We have also considered C_{Ga}-C_N-C_{Ga} complexes, which have been suggested to be a secondary source of high-wavenumber LVMs in heavily C-doped GaN.[25] Both the *pl* and *ax* configurations are shown in Fig. 2c and d. In each case, these complexes give rise to deep donor behavior, exhibiting a (2+/+) transition level (at 0.64 eV for *pl* and 0.45 eV for *ax*) as well as a (+/0) transition level (at 2.60 eV for *pl* and 2.88 eV for *ax*). For this complex we find significant relaxations away from the substitutional sites for one C_{Ga} member. In both the *pl* and *ax* configurations one C_{Ga} becomes three-fold coordinated, breaking a C−N bond, while the other C_N and C_{Ga} species remain in the vicinity of their substitutional sites.

The tricarbon C_{Ga}-C_i-C_N complex is stable in positively charged states over most of the GaN gap. It is stable in four charge states; 2+, +, 0, and 2−, and features three transition levels; a (2+/+) level at 1.48 eV, a (+/0) level at 2.47 eV, and a (0/2−) level 3.09 eV above the VBM. As can be seen in Fig. 2e, this complex resembles C_{Ga}-C_N, but with a C_i bridging between C_N and C_{Ga}. Both C_N and C_{Ga} are pushed slightly away from the substitutional sites, but maintain bonding with their three nearest neighbors (N atoms in the case of C_{Ga}, and Ga atoms in the case of C_N). C_i only forms bonds with the other two C atoms; these bond lengths vary from 1.36-1.50 Å (the smallest bond length for each charge state is reported in Table I).

In contrast, the tricarbon C_N-C_i-C_N complex is stable in only two charge states, 2+ and 0, and features a (2+/0) transition level 2.15 eV above the VBM. The structure of this complex (shown in Fig. 2f) is also distinct. It resembles the structure of the C_N-C_i complex, but with one second-nearest N neighbor replaced with a C atom. Thus although this complex exhibits formation energies that are among the lowest calculated for the tricarbon centers, it is unlikely to be a candidate for the tricarbon complex reported by Gamov et al.[25], which was claimed to have two distinct C−C bonds among three C atoms.

2. Binding energies of C complexes

We next consider the binding energies of complexes, which indicate their stability relative to the isolated members of each complex.[32] For calculating binding energies we specifically choose Fermi levels for which the complex formation process respects charge neutrality [for instance, $C_{Ga}^{+} + C_N^{-} \rightarrow (C_{Ga}\text{-}C_N)^0$, which we will consider for the dicarbon complexes]. This allows us to forgo considering the barriers associated with the exchange of carriers with the Fermi level (which may occur in processes that do not respect charge neutrality).[50] For the dicarbon complexes, such conditions occur when the Fermi level is 1 eV or higher above the VBM. Under this condition, we calculated a binding energy of −1.52 eV for the *ax* configuration and −1.65 eV for *pl*. These negative binding energies indicate that a complex is more stable than the individual constituents.

For the tricarbon complexes, we consider the charge-neutral process $(C_{Ga}\text{-}C_N)^0 + C_N^{-} \rightarrow (C_N\text{-}C_{Ga}\text{-}C_N)^{-}$, which could occur when the Fermi level is 1.5 eV or higher above the VBM. For this process we calculate a binding energy of −1.06 eV for the *ax* configuration and −1.20 eV for *pl*, which are lower than those of the dicarbon complexes. Coupled with their high formation energies, these results indicate that the formation of tricarbon complexes is not particularly favorable in thermodynamic equilibrium.[51] The C_{Ga}-C_N-C_{Ga} complexes also exhibit small binding energies. Again assuming the Fermi level is near 1.5 eV [and taking the process (C_{Ga}-

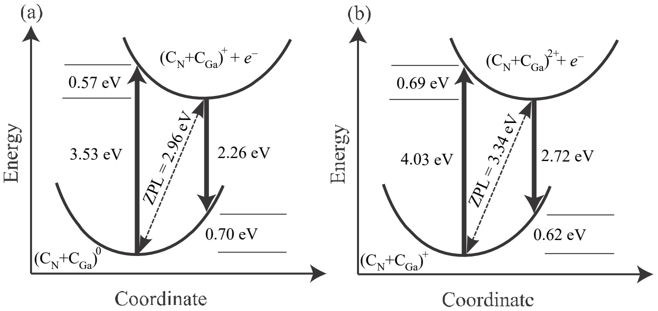

FIG. 6. Configuration coordinate diagrams for transitions involving the two charge-state transition levels of *pl* C_N-C_{Ga}. In (a), optical transitions for the (+/0) are shown, for which a PL peak of 2.26 eV and an absorption peak of 3.53 eV are calculated. In (b), transitions involving the (2+/+) level are shown, for which a PL peak of 2.72 eV and an absorption peak of 4.03 eV are calculated.

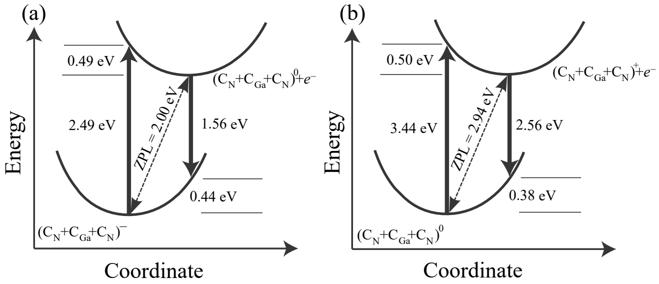

FIG. 7. Configuration coordinate diagrams for transitions involving the two charge-state transition levels of the C_N-C_{Ga}-C_N in its axial configuration. In (a), optical transitions for the (0/−) are shown, for which a PL peak of 1.93 eV and an absorption peak of 2.88 eV are calculated. In (b), transitions involving the (0/+) level are shown, for which a PL peak of 2.66 eV and an absorption peak of 3.50 eV are calculated.

$C_N)^0$ + $C_{Ga}^+ \rightarrow (C_N\text{-}C_{Ga}\text{-}C_N)^+$], we calculate a binding energy of −0.56 eV for the *ax* configuration and −0.83 eV for the *pl* configuration. In light of these small binding energies and large formation energies, we also find that the C_{Ga}-C_N-C_{Ga} complexes are unlikely to form.

By contrast, the C_{Ga}-C_i and C_N-C_i complexes have much larger binding energies. For C_N-C_i, assuming the Fermi level is ∼1 eV above the VBM, we consider the process $C_N^- + C_i^{2+} \rightarrow (C_N\text{-}C_i)^+$, which yields a binding energy of −2.75 eV. At the same Fermi level, and taking the process $C_{Ga}^+ + C_i^{2+} \rightarrow (C_{Ga}\text{-}C_i)^{3+}$, the binding energy of C_{Ga}-C_i is −3.75 eV. Coupled with its low formation energy for Fermi levels near the VBM, this binding energy indicates that the formation of this complex is favorable.

Finally we consider the remaining tricarbon complexes involving C_i: C_N-C_i-C_N and C_{Ga}-C_i-C_N. When the Fermi level is near 2.5 eV, charge neutrality can be maintained with the process $(C_N\text{-}C_i)^+ + C_N^- \rightarrow (C_N\text{-}C_i\text{-}C_N)^0$, for which we calculate a binding energy of −3.17 eV. For C_{Ga}-C_i-C_N we can take the Fermi level at 1 eV and consider the process $(C_{Ga}\text{-}C_N)^0 + C_i^{2+} \rightarrow (C_{Ga}\text{-}C_i\text{-}C_N)^{2+}$, for which we obtain a binding energy of −4.50 eV. Again, the relatively higher formation energies of these complexes (compared to C_{Ga}-C_i, for instance) indicates that they are not strongly favored, despite these large binding energies.

3. Optical properties of C-containing species

As stated in Sec. I, C_N has previously been calculated[12] to give rise to two PL bands, arising from its two thermodynamic transition levels [(+/0) and (0/−)]. The YL band, calculated to have a peak near 2.1 eV, is caused by electrons recombining into the (0/−) level, while the BL band, exhibiting a peak near 2.7 eV, is due to electrons recombining into the (+/0) level. Configuration-coordinate (CC) diagrams of these transitions are included in Ref. 12. We now consider optical transitions due to the C_N-C_{Ga} and C_N-C_{Ga}-C_N complexes, whose thermodynamic transition levels are similar to C_N, and might be expected to lead to the PL shift observed in Fig. 3. We construct CC diagrams for these complexes in Figs. 6 and 7 that are analogous to those previously reported in Ref. 12. In both cases we choose the lowest-energy configurations of each complex; optical transitions do not vary considerably between configurations of each type of defect.

Since C_N-C_{Ga} (*pl*) features two thermodynamic transition levels, we consider two sets of optical transitions (shown in Figs. 6a and b). Optical transitions related to the (+/0) level result in a PL peak at 2.26 eV [due to an electron recombining with $(C_N\text{-}C_{Ga})^+$] and absorption peaking at 3.53 eV [due to the excitation of an electron from $(C_N\text{-}C_{Ga})^0$ to the CBM], with a zero-phonon line (ZPL) at 2.96 eV. Optical transitions can also occur for the (2+/+) level, and are shown in Fig. 6b. We predict a PL peak at 2.72 eV [due to an electron recombining with $(C_N\text{-}C_{Ga})^{2+}$] and absorption peaking at 4.03 eV [due to the excitation of an electron from $(C_N\text{-}C_{Ga})^+$ to the CBM], with a ZPL at 3.34 eV. Relaxation energies for these optical transitions fall between 0.57 and 0.70 eV.

Similarly, two sets of optical transitions are calculated for the two thermodynamic transition levels of tricarbon C_N-C_{Ga}-C_N(*ax*), shown in Fig. 7. Again, two sets of optical transitions occur as these complexes feature two thermodynamic transition levels. For transitions involving the (0/−) level (Fig. 7a), we calculate a PL peak at 1.56 eV [due to an electron recombining with $(C_N\text{-}C_{Ga}\text{-}C_N)^0$] and absorption peaking at 2.49 eV [due to the excitation of an electron from $(C_N\text{-}C_{Ga}\text{-}C_N)^-$ to the CBM], with a ZPL at 2.00 eV. A very similar PL band was observed in highly C-doped GaN by Reuter et al. (Ref. 52) who observed a broad PL band with peak energy at 1.64 eV (when exciting with 2.4 eV light) and a photoluminescence excitation onset near 2 eV. Optical transitions for the (+/0) level (Fig. 7b) result in PL peaking at 2.56

eV [due to an electron recombining with $(C_N\text{-}C_{Ga}\text{-}C_N)^+$] and absorption peaking at 3.44 eV [due to the excitation of an electron from $(C_N\text{-}C_{Ga}\text{-}C_N)^0$ to the CBM], with a ZPL at 2.94 eV. For C_N-C_{Ga}-C_N the relaxation energies fall within 0.38-0.54 eV.

To summarize, the dicarbon C_N-C_{Ga} complex leads to a (+/0) thermodynamic transition level analogous to the (0/−) level of isolated C_N. Optical transitions associated with the (+/0) level of C_N-C_{Ga} are predicted to give rise to PL peaking at 2.26 eV, slightly blueshifted from the 2.13 eV PL peak calculated for optical transitions associated with the (0/−) level of C_N. Moreover, for the (2+/+) thermodynamic level of C_N-C_{Ga} [analogous to the (+/0) level of C_N], we predict an optical transition with a 2.72 eV PL peak that is similar to the 2.7 eV PL peak predicted previously for isolated C_N. Both the blueshifted YL peak and the mostly unshifted BL peak of C_N-C_{Ga} are consistent with the PL spectra observed in highly C-doped GaN shown in Fig. 3. In contrast, recombination into the (0/−) level of the tricarbon C_N-C_{Ga}-C_N complex is calculated to give rise to PL peaking at 1.56 eV, a strong redshift relative to the YL associated with isolated C_N. The PL peak calculated for the (+/0) level of C_N-C_{Ga}-C_N is 2.56 eV, which is also redshifted relative to the BL of C_N. Neither redshifted peak is consistent with the PL spectra shown in Fig. 3 for highly C-doped GaN.

With these results in hand, we can compare our calculations with the PL spectra shown in Fig. 3. We attribute the observed ∼0.1 blueshift in the peak of the "yellow" emission band (occurring with increasing C concentrations) to the emergence of another radiative recombination process involving the C_N-C_{Ga} dicarbon complex. For intermediate C concentrations, the broad "yellow" PL band is then likely comprised of the usual 2.1-2.2 eV emission band associated with the isolated C_N acceptor together with this new emission band, that is calculated to have a slightly higher peak energy of approximately 2.3 eV as shown in Fig. 6a. [Although the difference in calculated PL peaks associated with C_N and C_N-C_{Ga} is small (0.16 eV), it is larger than the usually quoted error bar in these calculations (0.1 eV)[32].] Subsequently, at the highest C concentration (10^{19} cm^{-3}), it then appears that the 2.3 "yellow" emission associated with the C_N-C_{Ga} complex becomes dominant. While the C_N-C_{Ga} deep donor complex will not be efficient at capturing holes, this could be consistent with the lower-intensity luminescence observed in the highly C-doped samples. Note also that even at these high C-doping levels, we do not exclude the possibility of a contribution to the PL in the "yellow" spectral region from the usual 2.23 eV emission band involving C_N deep acceptors.

We find that other low-energy centers are also unlikely to lead to PL peaks near the YL, and can likely be excluded from involvement in the optical transitions shown in Fig. 3. For instance, although C_i exhibits a (4+/2+) level at 0.67 eV (that is similar to the 0.9 eV acceptor level of C_N), optical transitions should occur for the transition levels involving only one charge carrier. However, neither the (4+/3+) level (at 1.96 eV above the VBM) nor the (3+/2+) level (that occurs 0.63 eV *below* the VBM) can give rise to optical transitions near the YL. The (2+/+) transition level of C_i occurs at 1.49 eV above the VBM, and thus recombination from an electron at the CBM into this level would have a ZPL of 2.01 eV. However, the relaxation energy for this process is 1.55 eV, giving a predicted PL peak of 0.46 eV, far from the YL peak.

C_N-C_i has a (3+/+) level at 0.78 eV. However, both the (3+/2+) level (at 2.10 eV above the VBM) and the (2+/+) level (at 0.55 eV *below* the VBM) have energies that preclude them from giving rise to a PL signal near the YL. Finally, we consider the C_{Ga}-C_i complex, which exhibits a (3+/2+) level at 1.59 eV above the VBM. This would imply a ZPL of 1.91 eV for transitions involving the recombination of an electron at the CBM. However, we calculate a relaxation energy of 0.63 eV for this process [i.e., $(C_{Ga}\text{-}C_i)^{3+} + e^- \rightarrow (C_{Ga}\text{-}C_i)^{2+}$], meaning that the associated PL transition would peak at 1.28 eV, far from the YL peak. Thus, among the carbon species and complexes investigated here, the dicarbon C_{Ga}-C_N complexes are the best candidates for explaining the shift in PL signals observed in highly C-doped GaN.

4. Vibrational modes of C-containing species

The four highest-wavenumber modes calculated for each stable charge state of each C species in GaN are listed in Table I. Most defects feature LVMs that vary considerably with their charge state. For instance, C_N^- features three modes in the range 751-763 cm^{-1}, which are quite similar to the 760-780 cm^{-1} LVMs recently attributed to the carbon acceptor.[10] (Similar modes were also observed in prior spectroscopic studies of C-doped GaN[53,54].) As electrons are removed from the C_N defect levels, these LVMs decrease, going from 500-714 cm^{-1} for the 0 charge state, to 439-556 cm^{-1} for the + charge state. The decreasing LVM energies occur as C−Ga bond lengths increase, going from 1.92 Å for C_N^- to 1.99 Å for C_N^+. We note that the C_N modes are distinct from those we calculate for C_{Ga}^+ (726-839 cm^{-1}); this was also observed by Wu et al. in Ref. 10.

Dicarbon C_N-C_{Ga} complexes give rise to wavenumbers higher than the isolated C_N and C_{Ga} species; again they vary with charge state. For $(C_N\text{-}C_{Ga})^0$, the LVMs vary between 769-942 cm^{-1} for the *pl* and *ax* configurations. These LVMs mostly shift higher as the complexes become more positive, to 720-970 cm^{-1} for $(C_N\text{-}C_{Ga})^+$ and 738-1112 cm^{-1} for $(C_N\text{-}C_{Ga})^{2+}$. Forming the tricarbon C_N-C_{Ga}-C_N complexes actually shifts these LVMs to lower wavenumbers, which stay mostly consistent for the three charge states of this center. For both *pl* and *ax* configurations, the LVMs fall within 738-969 cm^{-1} for the +, 0, and − charge states of C_N-C_{Ga}-C_N. The highest of these modes are outside the ranges of the LVMs reported by

TABLE I. LVMs and bond lengths for carbon-containing defects and complexes in GaN. All stable charge states for each defect are listed along with the shortest C-related bond length for each center (in Å), as well as the four highest-wavenumber modes (in cm^{-1}).

defect	state	bond (Å)	LVMs (cm^{-1})			
C_N	+	1.99	556	514	439	293
	0	1.95	714	659	500	292
	−	1.92	763	757	751	336
C_{Ga}	+	1.56	839	835	828	726
C_N-C_{Ga} (*ax*)	+	1.56	970	802	764	752
	0	1.58	932	814	809	779
C_N-C_{Ga} (*pl*)	2+	1.49	1112	871	850	796
	+	1.56	974	808	774	740
	0	1.57	942	812	810	769
C_N-C_{Ga}-C_N (*ax*)	+	1.44	1129	1088	896	790
	0	1.47	1134	1024	870	818
	−	1.47	1125	1005	867	785
C_N-C_{Ga}-C_N (*pl*)	+	1.45	1152	1086	772	722
	0	1.47	1141	1038	859	814
	−	1.47	1142	1028	848	776
C_{Ga}-C_N-C_{Ga} (*ax*)	2+	1.42	1079	1029	920	878
	+	1.43	1083	1013	909	871
	0	1.47	1023	934	871	853
C_{Ga}-C_N-C_{Ga} (*pl*)	2+	1.36	1224	1075	935	881
	+	1.36	1215	1075	936	866
	0	1.48	1014	935	896	870
C_i	4+	1.37	1302	1284	998	849
	2+	1.17	2247	438	322	319
	+	1.23	1851	674	515	419
	0	1.31	1539	745	706	461
	−	1.37	1336	917	885	515
C_N-C_i	3+	1.40	1235	1146	945	820
	+	1.23	2057	543	493	469
	0	1.29	1796	622	591	469
C_{Ga}-C_i	3+	1.34	1516	1325	1311	1166
	2+	1.35	1491	1277	1107	1086
	+	1.41	1471	1061	1044	992
	0	1.44	1357	1116	930	825
	−	1.45	1245	975	879	799
C_{Ga}-C_i-C_N	2+	1.36	1490	1304	1278	1126
	+	1.39	1471	1244	1085	1080
	0	1.41	1448	1107	1019	995
	−	1.44	1336	1089	935	805
	2−	1.47	1221	951	879	849
C_N-C_i-C_N	2+	1.29	1805	1202	713	700
	0	1.23	2052	782	771	735

Wu et al.[10] and Gamov et al.[25]

LVMs for the tricarbon complexes are slightly larger than those for the dicarbon complexes, and significantly higher than those for isolated C_N or C_{Ga}. This shift is consistent with the small C−C bond lengths for these tricarbon complexes, which are shorter than for those of the dicarbon complexes, C_N, or C_{Ga}. As the smallest bond lengths for these complexes do not strongly vary with charge state, neither do the highest-wavenumber LVMs for the *ax* and *pl* configurations of C_N-C_{Ga}-C_N, which vary between 1125-1152 cm^{-1}. The remaining lower-wavenumber modes fall within the range of 722-1088 cm^{-1}. Again, the highest of these modes are outside the ranges of the LVMs reported in previous studies of C-doped GaN.[10,25]

High-wavenumber LVMs are calculated for C_i, due to the C−N double bonds present when this center is a split interstitial. For these cases, C_i features a single high-wavenumber mode, due to the vibration of the C and N atoms that split the N site. This mode is highest for C_i^{2+} (2247 cm^{-1}) and decreases gradually (from 1851 cm^{-1} for the + charge state to 1336 for the − charge state) as electrons are added to the interstitial and its defect states are occupied. The lowest-wavenumber modes occur for C_i^{4+}, which does not exist as a split interstitial, but is octahedrally coordinated (and does not have a short C-N bond). C_i^{4+} exhibits LVMs between 849-1302 cm^{-1}.

The complexes containing C_i also feature similar high-wavenumber modes. For instance, C_N-C_i exhibits one LVM at 2057 cm^{-1} for its + charge state, which decreases to 1796 for the 0 and 1565 for the − charge state. The remaining LVMs fall between 469-810 cm^{-1} for each charge state. The high-wavenumber mode is again associated with vibrations originating from the C-C double bond. C_{Ga}-C_i also features a short C−C bond, that varies between 1.34-1.45 Å, depending on the charge state of this complex. The highest LVM, 1516 cm^{-1}, appears for the 2+ charge state (when this C−C bond is smallest). This mode decreases to its smallest value (1221^{-1}) for the − charge state of C_{Ga}-C_i (when this C−C bond is largest). We note that similar vibrational modes for C_i, C_{Ga}-C_i, and C_N-C_i were reported by Matsubara and Bellotti.[15] The C_{Ga}-C_i-C_N also shows this behavior, as the highest LVM varies between 1221-1490 cm^{-1}, taking its highest value when the bond length is smallest (1.36 Å in the 2+ charge state) and its smallest value when the C−C bond length is longest (1.47 Å in the 2− charge state). Although this complex has a high formation energy, it is the only tricarbon complex investigated here that has high LVMs and exhibits a structure similar to the one proposed by Gamov et al.[25]

Finally, the C_N-C_i-C_N complex has among the highest LVMs and shortest C−C bond lengths calculated in this study. In the 2+ charge state, the highest LVM is 1805 cm^{-1} and the shortest C−C bond length is 1.29 Å. This mode increases to 2064 cm^{-1} for the 0 charge state, as the C−C bond length decreases to 1.23 Å. Because this complex contains three C atoms, and has high LVMs in the vicinity of those observed by Gamov et al.,[25] it might be tempting to attribute it to the "tricarbon" complex observed in that study. However, as discussed above, the structure of this complex is quite distinct from that observed by Gamov et al. (e.g., there is no direct bonding for one C member to the other two), making this assignment unlikely.

IV. CONCLUSIONS

In conclusion, we have analyzed the properties of heavily C-doped GaN grown by HVPE using PL and ODMR, and examined the properties of multi-carbon complexes using first principles calculations. Multiple ODMR signals arising from the C_N acceptor are attributed to the two thermodynamic transition levels of this center. We also link these two signals to PL peaks observed in moderately C-doped GaN, the ∼2.9 eV blue and ∼2.2 eV yellow luminescence bands. PL experiments further show that C doping leads to a gradual blueshift of the YL peak, and a decrease in intensity of the BL peak.

Using hybrid DFT, we have investigated potential defect centers that could be present in heavily C-doped GaN, in particular defect complexes containing multiple C atoms. We find that the C_N-C_{Ga} complex, which has a stable binding energy, is the best candidate for explaining the observed optical signals. We attribute the ∼0.1 eV blueshift of the "yellow" emission band peak energy with increasing C concentration to the emergence of another radiative recombination process involving the C_{Ga}-C_N complex. For intermediate C concentrations, the broad "yellow" PL is likely comprised of the usual 2.2 eV emission band (associated with isolated C_N) and this new emission band that is calculated to have a slightly higher ZPL energy. Most notably, it appears that the "yellow" emission associated with C_{Ga}-C_N is dominant for the highest C concentrations (10^{19} cm^{-3}).

Furthermore, the C_{Ga}-C_i complex is identified as a low-formation-energy complex with a high binding energy that may be a compensating donor in C-doped GaN. We also calculate LVMs associated with the C-containing complexes, in light of recent experiments that attribute vibrational modes above 1600 cm^{-1} to tricarbon C_N-C_{Ga}-C_N complexes. Our calculations that such tricarbon centers lead to LVMs below 1000 cm^{-1} that are only moderately larger than those related to isolated C_{Ga} or C_N. Instead, we find that complexes containing C_i, which lead to modes above 1500 cm^{-1}, are better candidates for explaining such signals.

V. ACKNOWLEDGEMENTS

Support for work at NRL was provided by the Office of Naval Research through the Naval Research Laboratory's Basic Research Program. Work at the Institute of High Pressure Physics was funded by the TEAM TECH program of the Foundation for Polish Science, co-financed by the European Union under the European Regional Development Fund (No. POIR.04.04.00-00-5CEB/17-00). The work at UAB is supported by NSF/DMR-1904325. Subash Paudel is supported by ULTRA, an Energy Frontier Research Center, funded by the U.S. Department of Energy, Office of Basic Energy Sciences, Materials Sciences and Engineering Division under Award No. DE-SC0021230. Computations were performed at the DoD Supercomputing Resource Center at ARL. We thank Prof. Chris G. Van de Walle for fruitful discussions.

[1] A. Wickenden, D. Koleske, R. Henry, M. Twigg, and M. Fatemi, J. Crys. Growth **260**, 54 – 62 (2004).

[2] C. Ozgit-Akgun, E. Goldenberg, A. K. Okyay, and N. Biyikli, J. Mater. Chem. C **2**, 2123–2136 (2014).

[3] C. Poblenz, P. Waltereit, S. Rajan, S. Heikman, U. K. Mishra, and J. S. Speck, J. Vac. Sci. Technol. B **22**, 1145–1149 (2004).

[4] S. W. Kaun, M. Hoi Wong, J. Lu, U. K. Mishra, and J. S. Speck, Electron. Lett. **49**, 893 (2013).

[5] T. Kogiso, T. Narita, H. Yoshida, Y. Tokuda, K. Tomita, and T. Kachi, Jpn. J. Appl. Phys. **58**, SCCB36 (2019).

[6] N. Remesh, N. Mohan, S. Raghavan, R. Muralidharan, and D. N. Nath, IEEE Trans. Electron Dev. **67**, 2311–2317 (2020).

[7] E. Fabris, C. De Santi, A. Caria, K. Mukherjee, K. Nomoto, Z. Hu, W. Li, X. Gao, H. Marchand, D. Jena, H. G. Xing, G. Meneghesso, E. Zanoni, and M. Meneghini, IEEE Transactions on Electron Devices , 1–5 (2020).

[8] J. L. Lyons, A. Janotti, and C. G. Van de Walle, Appl. Phys. Lett. **97**, 152108 (2010).

[9] M. Iwinska, R. Piotrzkowski, E. Litwin-Staszewska, T. Sochacki, M. Amilusik, M. Fijalkowski, B. Lucznik, and M. Bockowski, Appl. Phys. Express **10**, 011003 (2016).

[10] S. Wu, X. Yang, H. Zhang, L. Shi, Q. Zhang, Q. Shang, Z. Qi, Y. Xu, J. Zhang, N. Tang, X. Wang, W. Ge, K. Xu, and B. Shen, Phys. Rev. Lett. **121**, 145505 (2018).

[11] T. Ogino and M. Aoki, Jap. J. Appl. Phys. **19**, 2395 (1980).

[12] J. L. Lyons, A. Janotti, and C. G. Van de Walle, Phys. Rev. B **89**, 035204 (2014).

[13] M. A. Reshchikov, M. Vorobiov, D. O. Demchenko, U. Özgür, H. Morkoç, A. Lesnik, M. P. Hoffmann, F. Hörich, A. Dadgar, and A. Strittmatter, Phys. Rev. B **98**, 125207 (2018).

[14] T. Narita, K. Tomita, Y. Tokuda, T. Kogiso, M. Horita, and T. Kachi, J. Appl. Phys. **124**, 215701 (2018).

[15] M. Matsubara and E. Bellotti, J. Appl. Phys. **121**, 195701 (2017).

[16] M. Matsubara and E. Bellotti, J. Appl. Phys. **121**, 195702 (2017).

[17] P. Deák, M. Lorke, B. Aradi, and T. Frauenheim, Phys. Rev. B **99**, 085206 (2019).

[18] M. E. Zvanut, S. Paudel, E. R. Glaser, M. Iwinska, T. Sochacki, and M. Bockowski, J. Electron. Mat. **48**, 2226–2232 (2019).

[19] R. Piotrzkowski, M. Zajac, E. Litwin-Staszewska, and M. Bockowski, Appl. Phys. Lett. **117**, 012106 (2020).

[20] K. Irmscher, C. Hartmann, C. Guguschev, M. Pietsch, J. Wollweber, and M. Bickermann, J. Appl. Phys. **114**, 123505 (2013).

[21] K. Irmscher, I. Gamov, E. Nowak, G. Gärtner, F. Zimmermann, F. C. Beyer, E. Richter, M. Weyers, and G. Tränkle, Appl. Phys. Lett. **113**, 262101 (2018).

[22] E. Richter, F. C. Beyer, F. Zimmermann, G. Gärtner, K. Irmscher, I. Gamov, J. Heitmann, M. Weyers, and G. Tränkle, Crys. Res. Technol. **55**, 1900129 (2019).

[23] I. Gamov, C. Hartmann, J. Wollweber, A. Dittmar, T. Straubinger, M. Bickermann, I. Kogut, H. Fritze, and K. Irmscher, J. Appl. Phys. **126**, 215102 (2019).

[24] I. Levine, I. Gamov, M. Rusu, K. Irmscher, C. Merschjann, E. Richter, M. Weyers, and T. Dittrich, Phys. Rev. B **101**, 245205 (2020).

[25] I. Gamov, E. Richter, M. Weyers, G. Gärtner, and K. Irmscher, J. Appl. Phys. **127**, 205701 (2020).

[26] W. Kohn and L. J. Sham, Phys. Rev. **140**, A1133 (1965).

[27] J. Heyd, G. E. Scuseria, and M. Ernzerhof, J. Chem. Phys. **118**, 8207 (2003).

[28] J. Heyd, G. E. Scuseria, and M. Ernzerhof, J. Chem. Phys. **124**, 219906 (2006).

[29] G. Kresse and J. Furthmüller, Phys. Rev. B **54**, 11169 (1996).

[30] P. E. Blöchl, Phys. Rev. B **50**, 17953–17979 (1994).

[31] H. Monkhorst and J. Pack, Phys. Rev. B **13**, 5188–5192 (1976).

[32] C. Freysoldt, B. Grabowski, T. Hickel, J. Neugebauer, G. Kresse, A. Janotti, and C. G. Van de Walle, Rev. Mod. Phys. **86**, 253–305 (2014).

[33] C. Freysoldt, J. Neugebauer, and C. G. Van de Walle, Phys. Rev. Lett. **102**, 016402 (2009).

[34] C. Freysoldt, J. Neugebauer, and C. G. Van de Walle, Phys. Status Solidi B **248**, 1067–1076 (2011).

[35] J. L. Lyons, D. Wickramaratne, and C. G. Van de Walle, J. Appl. Phys. **129**, 111101 (2021).

[36] M. Bockowski, M. Iwinska, M. Amilusik, B. Lucznik, M. Fijalkowski, E. Litwin-Staszewska, R. Piotrzkowski, and T. Sochacki, J. Cryst. Growth **499**, 1–7 (2018).

[37] D. S. Green, U. K. Mishra, and J. S. Speck, J. Appl. Phys. **95**, 8456 (2004).

[38] R. Armitage, Q. Yang, and E. R. Weber, J. Appl. Phys. **97**, 073524 (2005).

[39] Z.-Q. Fang, D. C. Look, B. Claflin, S. Haffouz, H. Tang, and J. Webb, Phys. Stat. Sol. (c) **2**, 2757 (2005).

[40] F. Brunner, E. Bahat-Treidel, M. Cho, C. Netzel, O. Hilt, J. Würfel, and M. Weyers, Phys. Stat. Sol. (c) **8**, 2427 (2011).

[41] W. E. Carlos, J. A. Freitas, Jr., M. A. Khan, D.T. Olson, and J.N. Kuznia, Phys. Rev. B **48**, 17878 (1993).

[42] E. R. Glaser, T. A. Kennedy, K. Doverspike, L. B. Rowland, D. K. Gaskill, J. A. Freitas, Jr., M. Asif Khan, D. T. Olson, J. N. Kuznia, and D. K. Wickenden, Phys. Rev. B **51**, 13326 (1995).

[43] D. M. Hofmann, D. Kovalev, G. Steude, B. K. Meyer, A. Hoffmann, L. Eckey, R. Heitz, T. Detchprom, H. Amano, and I. Akasaki, Phys. Rev. B **52**, 16702 (1995).

[44] U. Kaufmann, M. Kunzer, C. Merz, I. Akasaki, and H. Amano, Mater. Res. Symp. Proc. **395**, 633 (1996).

[45] F. K. Koschnick, K. Michael, J.-M. Spaeth, B. Beaumont, and P. Gibart, Phys. Rev. B **54**, R11042 (1996).

[46] P. W. Mason, G. D. Watkins, and A. Dornen, Mater. Res. Symp. Proc. **449**, 793 (1997).

[47] C. E. Dreyer, A. Alkauskas, J. L. Lyons, and C. G. Van de Walle, Phys. Rev. B **102**, 085305 (2020).

[48] S. Limpijumnong, X. Li, S.-H. Wei, and S. B. Zhang, Appl. Phys. Lett. **86**, 211910 (2005).

[49] A. J. E. Rowberg, L. Weston, and C. G. Van de Walle, ACS Appl. Ener. Mater. **2**, 2611–2619 (2019).

[50] Q. Yan, A. Janotti, M. Scheffler, and C. G. Van de Walle, Appl. Phys. Lett. **100**, 142110 (2012).

[51] C. G. Van de Walle and J. Neugebauer, J. Appl. Phys. **95**, 3851–3879 (2004).

[52] E. E. Reuter, R. Zhang, T. F. Kuech, and S. G. Bishop, MRS Internet J. Nitride Semicond. Res. **4**, 363 (1999).

[53] M. F. Cerqueira, L. G. Vieira, A. Alves, R. Correia, M. Huber, A. Andreev, A. Bonanni, and M. I. Vasilevskiy, J. Phys. D: Appl. Phys. **50**, 365103 (2017).

[54] S. Ito, H. Kobayashi, K. Araki, K. Suzuki, N. Sawaki, K. Yamashita, Y. Honda, and H. Amano, J. Cryst. Growth **414**, 56 – 61 (2015).